Proceedings of the Eighth Meeting of the International Collaboration on Advanced Neutron Sources (ICANS-VIII)
8-12 July 1985, Rutherford Appleton Laboratory Report RAL-85-110

STATUS OF THE LOS ALAMOS ANGER CAMERA

P. A. Seeger and M. J. Nutter
Los Alamos National Laboratory, Los Alamos, NM 87545, U.S.A.

Abstract

Results of preliminary tests of the neutron Anger camera being developed at Los Alamos are presented. This detector uses a unique encoding scheme involving parallel processing of multiple receptive fields. Design goals have not yet been met, but the results are very encouraging and improvements in the test procedures are expected to show that the detector will be ready for use on a small-angle scattering instrument next year.

1. Introduction

The Anger camera, originally invented for use as a gamma-ray imaging detector for medical applications [1], has been successfully adapted for neutron use at the Argonne National Laboratory [2]. The Los Alamos version differs significantly in its encoding scheme [3]. Fig. 1 is a diagram of a detector with 13 photomultipliers (PMs). Scintillating material is placed in front of only the central PMs, however. An optical glass dispersing plate allows the photons from a neutron capture event to reach a group of seven PMs (a "receptive field"), in varying amounts depending on where the event was. The detector illustrated has three overlapping receptive fields. The linear combinations of signals which determine the position within each field are formed in parallel for all fields in the camera. Position determination is then a two-step process: first, determine which field, and second, interpolate within the field. Since the precision needed for the interpolation is much less than that needed in the standard Anger camera to find a centroid over the entire active area, the electronics may be much faster. The total encoding time per event in our present detector is 400 ns. Furthermore, in a large detector it is possible to analyze events simultaneously in different fields, and so the counting rate may be very high.

The present prototype detector at Los Alamos has 29 PMs and 13 receptive fields. The active area is 150 mm x 255 mm.

2. Calibration

Our present problems with the camera stem largely from lack of an adequate calibration procedure. It is essential that all PMs have the same gain, which is usually accomplished by adjusting the individual high voltages. The calibration and the subsequent tests described here were done using a monochromatic (1.257 Å) neutron beam from the Omega West Reactor at Los Alamos. We have made a mask, 1-cm thick, filled with ^{10}B powder, with ten circular plugs of Aℓ to provide neutron spots 6 mm in diameter at precisely determined positions. (See fig. 2.) By reflecting the mask about the horizontal and vertical centerlines and using all four orientations, 29 unique beam positions are defined. We attempt to adjust the PM gains till the pulse height spectra are the same for all 29 readings. Unfortunately, since the scintillator does not extend over the peripheral PMs, the observed signals do not have a one-to-one correspondance with the photomultiplier gains. At best, we can assure that the linear combinations we measure are linearly independent, so that we can invert a 29 x 29 matrix to find the adjustments. Our matrix does not converge very rapidly, however, and does not behave well when one PM is sick, or has bubbles in its optical coupling grease, etc.

For the tests reported here, the calibration had been carried through 3 iterations, but it was clear that at least one photomultiplier was not responding properly, and that our matrix had inadequate sensitivity to determine the extreme top and bottom PM gains. Thus the following tests were carried out under conditions far from optimum.

3. Test Procedure and Results

The camera was mounted on a translation stage driven by a stepping motor. The mask (described above) was mounted in a fixed position, so that only one of its apertures was illuminated by the neutron beam. The camera was set to an arbitrary height and a scan was made in the X-direction, as shown in fig. 3. The translation motor was driven 1000 steps (5 mm) and neutrons were counted for 100 s. The data were stored in a LeCroy 3588 histogramming memory at data rates of about 10000 s^{-1}. After completing the X traverse the camera was turned on its side and the Y scan was made.

Since the memory was not large enough to hold a histogram with full resolution in both dimensions simulataneously, the camera's encoder was set to record only 7 bins in the transverse dimension, and the full resolution capability (1.15 mm per bin) in the direction of interest. Data were subsequently summed in the transverse direction, so the entire detector area contributed to the background. (No background subtraction was made, but only the data near the peak were used in determining the second moment.) The quantities to be determined were uniformity of count rate, linearity of position encoding, and resolution of the spot as a function of position.

The results of these two scans are summarized in fig. 4. The uniformity, or integrated intensity, is most affected by the gain calibration of the PMs. We note a dip at Y = 225 mm, corresponding to the portion of the scan in field 24. We subsequently discovered that the PM in the upper left corner of field 24 was not completely optically coupled. The dip at X = 60 mm corresponds to the triple-point between fields 0, 1, and 9, and probably resulted from events being analyzed in field 9 when they should have been in field 1. If we neglect the one bad X point, the rms uniformity is 3%, which we confidently expect to improve with better calibration. Remembering that the spot size was 6 mm, the linearity and the resolution results are surprisingly good. (The known variance of the circular spot was subtracted from the calculated second moments to estimate the standard deviations.) There are features in the linearity plots at the same places that the count rate was low. Both linearity and resolution require that the position determination be continuous as we cross from one field to the next. There is only a single global adjustment available for all field overlaps in the entire camera; these scans give our first indication that one knob is enough.

4. Future Improvements

The alumina powder reflector on the scintillator glass had partially separated, and also may have contributed to a background pedestal around each reading. We have now aluminized that surface of the glass; Monte-Carlo simulations indicate this may also increase our position sensitivity slightly.

A revised calibration scheme is being developed. We propose first to adjust the 13 PMs over which we can center the beam, and then to use a 16 x 16 matrix of readings for the others.

For complete testing, it is obviously necessary to take many scans in each direction, rather than one. We must improve the automation of our data collection system to make this practical.

This prototype detector will be installed on the LQD flight path for further testing this fall. We will then be prepared to test for two other properties of the Anger camera, which must be answered before we can commit to using it in the final LQD instrument. These are stability (both short term and long term), and gamma-ray response in the environment of the pulsed source.

Acknowledgments

We greatly appreciate the cooperation we have had in this project from M. G. Strauss and his co-workers at Argonne, and from R. Lawrence and others from Rutherford Appleton Laboratories. This work was performed under the auspices of the U. S. Department of Energy, Office of Basic Energy Science.

References

[1] H.O. Anger, Rev. Sci. Instr. **29** (1958) 27.

[2] M.G. Strauss, R. Brenner, F.J. Lynch and C.B.Morgan, IEEE Trans. Nucl Sci. **NS28** (1981) 800.

[3] P.A. Seeger, IEEE Trans. Nucl. Sci. **NS31** (1984) 274.

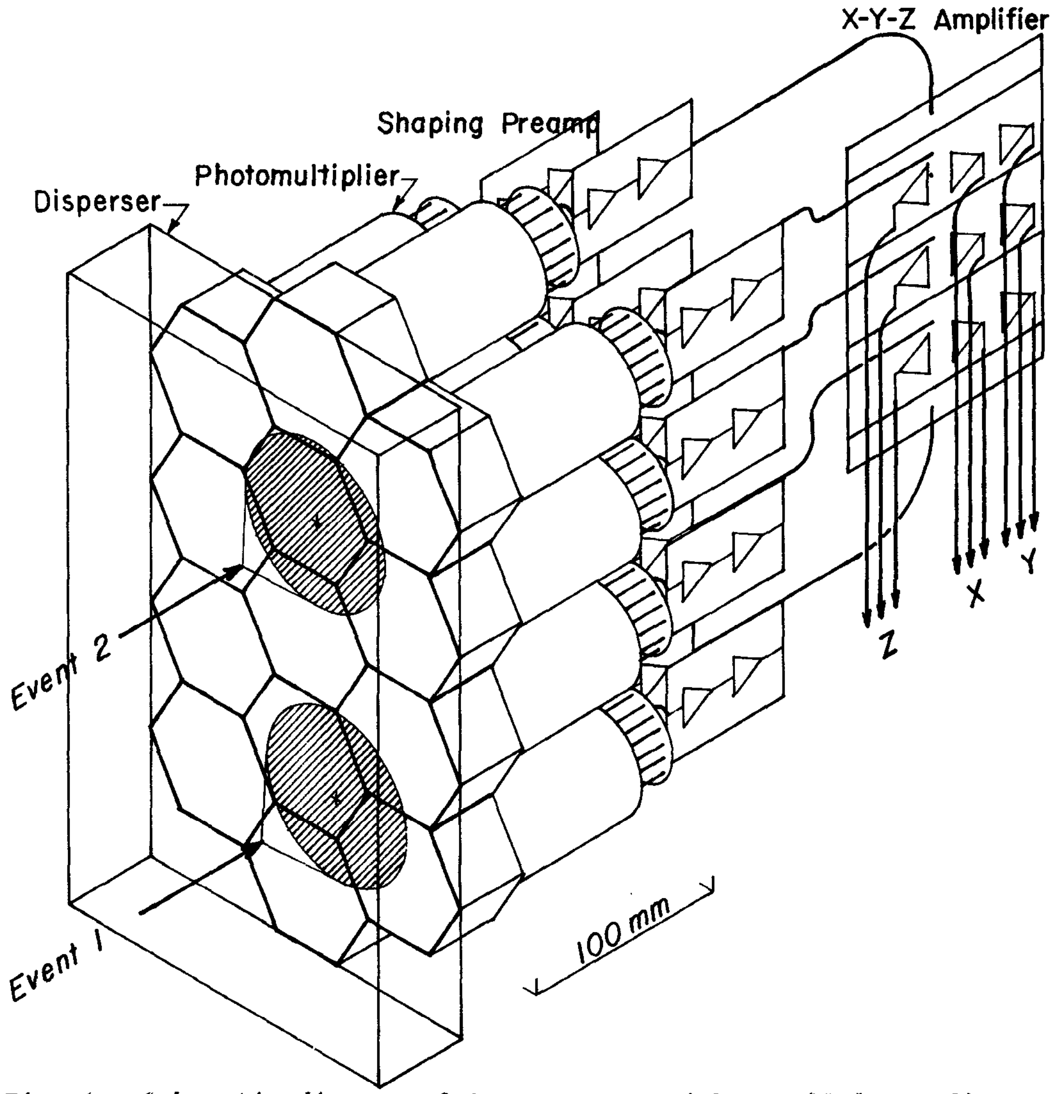

Fig. 1. Schematic diagram of Anger camera with parallel encoding. Encoding is done in two steps: choice of one of the possible receptive fields, and interpolation within the field.

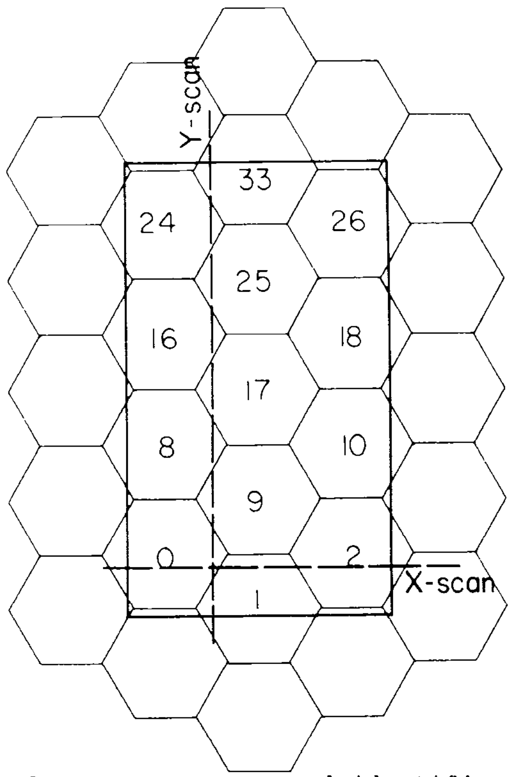

Fig. 3. Locations of X any Y scans, and identification of receptive fields.

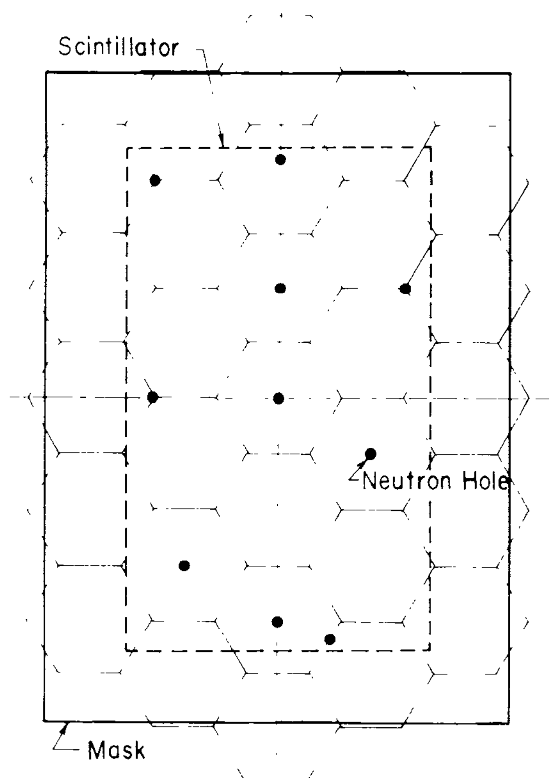

Fig. 2. Mask for calibration of photomultiplier gains. Reflections about horizontal and vertical axes result in 29 unique beam positions, to be used to determine the 29 gains.

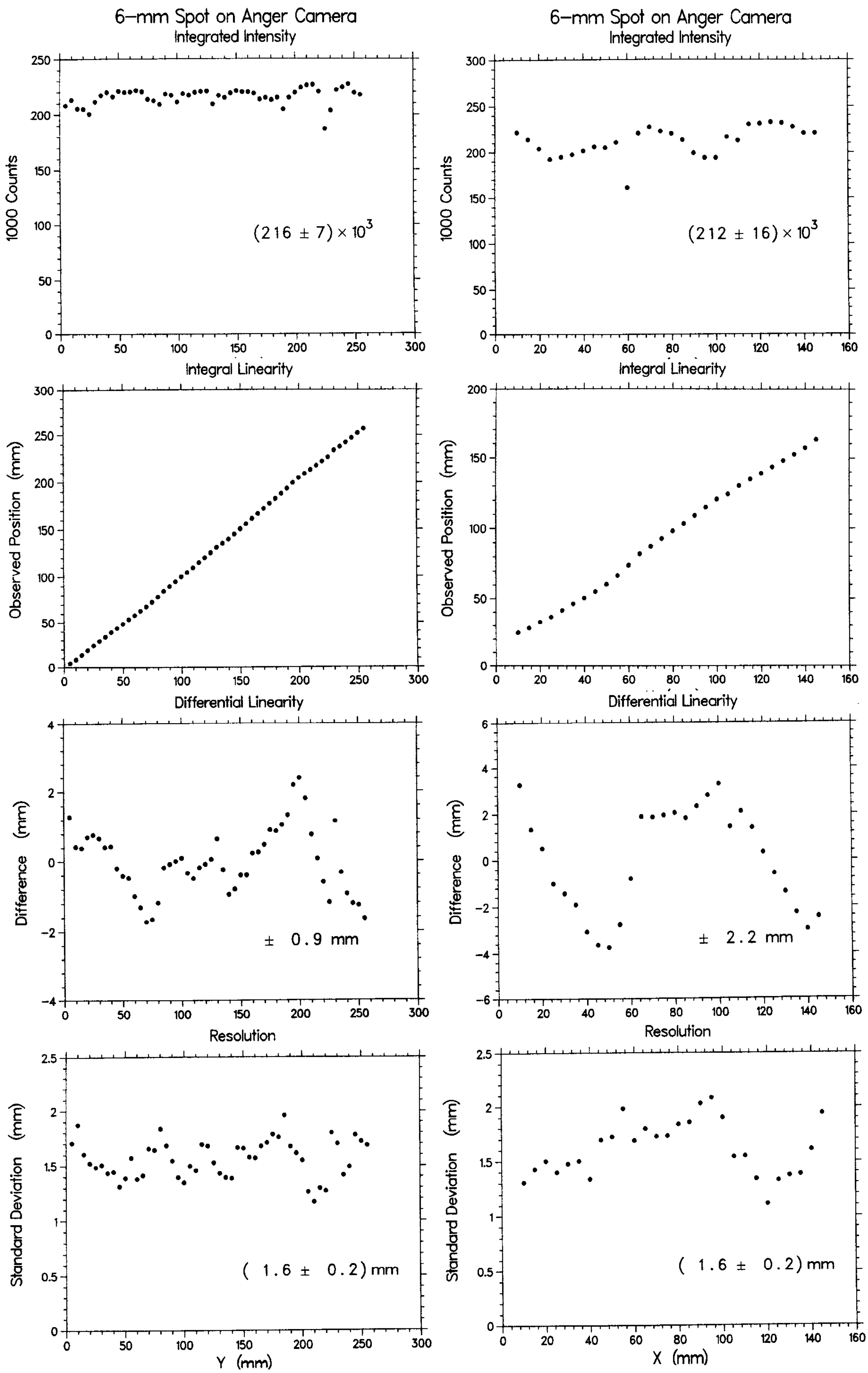

Fig. 4. Test Results